Fingering pattern induced by spinodal decomposition in hydrodynamically stable displacement in a partially miscible system

Ryuta X. Suzuki, Yuichiro Nagatsu, Manoranjan Mishra, and Takahiko Ban

Phys. Rev. Fluids **4**, 104005 — Published 29 October 2019

DOI: 10.1103/PhysRevFluids.4.104005

Fingering pattern induced by spinodal decomposition in hydrodynamically stable displacement in a partially miscible system

Ryuta X. Suzuki[1], Yuichiro Nagatsu[1,2*], Manoranjan Mishra[3,4**], Takahiko Ban[5***]

*e-mail: nagatsu@cc.tuat.ac.jp

**e-mail: manoranjan@iitrpr.ac.in

***e-mail: ban@cheng.es.osaka-u.ac.jp

1 Department of Chemical Engineering, Tokyo University of Agriculture and Technology, 2-24-16, Koganei, Tokyo, 184-8588, Japan

2 PRESTO, Japan Science and Technology Agency, Saitama, 332-0012, Japan

3 Department of Mathematics, Indian Institute of Technology Ropar, Rupnagar, 140001, India

4 Department of Chemical Engineering, Indian Institute of Technology Ropar, Rupnagar, 140001, India

5 Division of Chemical Engineering, Department of Materials Engineering Science, Graduate School of Engineering Science, Osaka University, 1-3, Machikaneyamacho, Toyonaka, Osaka, 560-8531, Japan

The dynamics of the displacement of one fluid by another in porous media or Hele-Shaw cells depends on the viscosity contrast due to Saffman–Taylor instability. If the less viscous fluid is displaced by the more viscous one, the interface is hydrodynamically stable, and thus, fingering does not occur. Herein, we experimentally show the occurrence of fingering for hydrodynamically stable displacement in a partially miscible system using an aqueous two-phase system. Quantitative correlation between the interfacial deformation and a newly proposed dimensionless number demonstrates that body force driven by spinodal decomposition induces the fingering instability. Moreover, the fingering observed in this study is completely different from previously reported fingering phenomena in hydrodynamically stable displacement in immiscible and fully miscible systems.

I. Introduction

The displacement of one fluid by another in porous media is observed in several processes such as chromatographic separation [1], CO_2 sequestration [2], and secondary and tertiary oil recovery [3]. When the displaced fluid is more viscous than the displacing one, the interface is hydrodynamically unstable and forms finger-like patterns owing to a positive viscosity gradient in the flow direction; this reduces the displacement efficiency. Such a finger-like pattern is called viscous fingering (VF) [4–6], and the dynamics of VF have been extensively investigated in extant studies [7,8]. VF is generally divided into two categories depending on whether two fluids are immiscible or fully miscible. The solubility between two fluids is negligible in an immiscible system and infinite in a fully miscible system. If the viscosity contrast and flow rate are identical, the typical finger width in an immiscible system is larger than that in a fully miscible system because of higher interfacial tension [9,10]. Studies have investigated the influences of non-Newtonian fluid properties [11–14] and several physicochemical effects between two fluids, such as those corresponding to chemical reactions [15–21], double diffusivity [22], and phase change [23], on VF dynamics. These studies primarily used a Hele-Shaw cell; this cell has a thin gap between two parallel plates, and it is the simplest two-dimensional model of a porous medium [7].

In contrast, when the displaced fluid is less viscous, the interface is hydrodynamically stable and grows uniformly because of the negative viscosity gradient in the flow direction. We have focused on the previously reported occurrence of fingering instability induced by several physicochemical effects even under such hydrodynamically stable conditions in immiscible and fully miscible systems [22,24–35]. Chan and Liang [24] discovered such fingering in an immiscible system formed during displacement of air by a surfactant solution in a Hele-Shaw cell whose inner surface was prewetted by the surfactant solution. This fingering was attributed to solutal capillary convection induced by spatial variation of the surfactant concentration [28,29]. Bihi et al. [30] observed such fingering in an immiscible system—displacement of air by water in a Hele-Shaw cell—in which partially wettable hydrophilic particles were present and demonstrated that it originated due to capillary force induced by preexisting particles. In fully miscible systems, experimental and numerical analyses have shown that a local positive viscosity gradient established by viscosity change due to chemical reaction [31–34] or a local negative permeability gradient established by precipitation reaction [35] both induce such fingering in standard Hele-Shaw cells that are not subjected to any pretreatment. Furthermore, the establishment of a local viscosity gradient responsible for such fingering by double diffusivity in the fully miscible system has been numerically predicted [22]. The other reported origin for the establishment of a local viscosity gradient is accumulation of particles when a more viscous suspension, in which particles are dispersed, displaces less viscous air in a standard Hele-Shaw cell [25–27].

Recently, studies have focused on fluid displacement in partially miscible systems, where the

fluids have finite solubility at the interface [36–38], mainly because fluids are partially miscible under the reservoir condition at high pressure in the CO_2-enhanced oil recovery (EOR) process [39]. Thus far, hydrodynamically unstable displacement in partially miscible systems has mostly been studied through numerical simulations [36–38]. One numerical simulation [38] showed that partial miscibility greatly influences the degree of fingering. However, the fingering in partially miscible system has not been investigated experimentally because little has been known how to control the miscibility at room temperature and atmospheric pressure.

In the present study, we have succeeded in experimentally changing the solution system from fully miscible to partially miscible or immiscible by varying the concentrations of the components in an aqueous two-phase system (ATPS) while leaving the viscosities relatively unchanged at room temperature and atmospheric pressure. We conduct a hydrodynamically stable displacement experiment in which a more viscous fluid displaces a less viscous one in a radial Hele-Shaw cell by using ATPS. The results showed that fingering instability occurs even under hydrodynamically stable conditions only in the partially miscible system. We aim to clarify the origin of such fingering.

II. Solution System and Displacement Experiment

We use an ATPS consisting of polyethylene glycol (PEG; weight-average molecular weight M_w = 8000), a salt (Na_2SO_4), and water [40]. Figure 1(a) shows the phase diagram, where the blue region indicates that the system consists of one phase and the green region indicates that the system has separated into two phases. An aqueous solution composed of 13% w/w Na_2SO_4 and 10% w/w PEG (red triangle point in Fig. 1(a)) is separated into a PEG-rich phase (phase L, lighter phase; Na_2SO_4 and PEG compositions are 3.2% w/w and 36.5% w/w, respectively; red filled circle) and a salt-rich phase (phase H, heavier phase; Na_2SO_4 and PEG compositions are 16.0% w/w and 1.4% w/w, respectively; red open circle) [40]. In all displacement experiments, the more viscous PEG-rich solution displaces the less viscous salt-rich solution. Both phases after equilibrium are used in the immiscible system. The system can be changed from fully miscible to partially miscible by increasing only the salt concentration, C_s, of the displaced solution when 36.5% w/w PEG solution (black filled circle) is used as the displacing solution. When the average concentrations of PEG and Na_2SO_4 after mixing equal volumes of PEG and Na_2SO_4 solutions as more- and less- viscous solutions, respectively, lie in Region I, the system becomes fully miscible. When they lie in the thermodynamically unstable region, Region II, the system becomes partially miscible with finite solubility where phase separation occurs due to spinodal decomposition. When C_s = 0% w/w (deionized water; black open circle), the average concentrations become 18.25% w/w PEG and 0% w/w Na_2SO_4 (black filled star) and lie in Region I; the system is fully miscible. In contrast, when C_s = 20% w/w (green open circle), the average concentrations become 18.25% w/w PEG and 10% w/w Na_2SO_4 (green filled star) and lie in Region II; the system is partially miscible. The fully and

partially miscible systems are in nonequilibrium. Thus, the change in their compositions occurs during displacement. As shown in Table 1, the viscosities of the more and less viscous solutions are relatively unchanged for all systems.

In all displacement experiments, the more viscous solution is dyed in blue using indigo carmine to visualize the displacement pattern. We have confirmed that indigo carmine is not soluble in the Na_2SO_4 solution because of the salting-out effect. The gap of the Hele-Shaw cell, b, is 0.3 mm. The injection flow rate of the more viscous liquid, q, is varied between q_0 and $13q_0$ ($q_0 = 7.07 \times 10^{-10}$ m^3/s).

III Results and Discussion

Figure 1(b) shows the displacement patterns for immiscible (phase L−phase H system), fully miscible (36.5% w/w PEG–0% w/w Na_2SO_4 system), and partially miscible (36.5% w/w PEG–20% w/w Na_2SO_4 system) systems for the lowest q ($=q_0$). Hydrodynamically stable interfaces are observed in both the immiscible and the fully miscible cases. The fully miscible interface is observed to be not sharp due to diffusion, which is different from that in the immiscible case. However, in the partially miscible case, a noncircular deformed interface appears. Figure 1(c) shows the temporal growth of the pattern for all systems for $q = q_0$. For immiscible and fully miscible systems, the patterns are circular regardless of time. The deformed pattern can be clearly visible after $t = 1000$ s, and the deformation becomes larger as time progresses for the partially miscible system.

As described in the introduction, some fingering instabilities even under hydrodynamically stable conditions are attributed to the establishment of a local positive viscosity gradient [25–27,31–34]. To check whether such a local positive viscosity gradient is established, we measure the viscosity in the interfacial region for each system by performing interfacial rheological measurements using a rheometer (AR-G2, TA Instruments) with a double-wall ring-type sensor [41]. In the measurement, we first put the heavier solution in the vessel and then set the ring at the air-solution interface. Here, the heavier solution refers to 36.5 % w/w PEG solution in fully miscible system, phase H in immiscible system, and 20 % w/w Na_2SO_4 solution in partially miscible system. Then, we start small amplitude oscillatory shear measurement at fixed frequency (0.20 Hz) and strain (1.0 %). Figure 2(a) shows the temporal evolutions of G' (storage modulus) and G'' (loss modulus), which represent elastic and viscous responses, respectively, for the immiscible, fully miscible, and partially miscible systems. At $t = 180$ s (indicated by a blue solid line in Fig. 2(a)), the lighter solution (0 % w/w Na_2SO_4 solution in fully miscible system, phase L in immiscible system, and 36.5 % w/w PEG solution in partially miscible system) is added, bringing the two phases into contact with each other. The initial time up to 180 s (showed at the blue line in Fig.2(a) in the manuscript) is not our interest because a liquid-air interface is measured before 180 s and a liquid-liquid interface is measured after 180 s when two solutions are brought into contact with each

other. In all cases, the values of G' are dispersed, indicating that G' is too small to be measured and that the elastic properties are negligible. Meanwhile, G'' is constant with time in all cases. In other words, the viscosity in the interfacial region is constant within the experimental period. Thus, it can be concluded that the deformation occurring in the partially miscible system is not triggered by the establishment of a local viscosity gradient.

We measure the temporal change in interfacial tension, γ, for the immiscible, fully miscible, and partially miscible systems by using a spinning drop tensiometer (SITE 100, Krüss, Germany) [42,43]. Note that 9% w/w Na_2SO_4 solution is used instead of 0% w/w Na_2SO_4 solution for the fully miscible system because the measurement cannot be performed for the 36.5% w/w PEG–0% w/w Na_2SO_4 system due to extremely low interfacial tension. As shown in Fig. 2(b), as expected, γ remains constant with time for the immiscible system and it decreases with time for the fully miscible system; interestingly, γ increases with time for the partially miscible system.

Here, we propose an origin of the interfacial deformation in a partially miscible system in terms of chemical thermodynamics. In this study, we thermodynamically control the miscibility of two aqueous solutions by varying the concentration of salt. When the two solutions are in contact with each other far from the thermodynamic equilibrium, the compositions at the interface between the two solutions changes due to mass transfer depending on the difference between the initial and the equilibrium free energies; this leads to a concentration gradient at the interface. The reference [44] theoretically shows that spinodal decomposition makes concentration gradient steeper. Based on this reference, for a partially miscible system passing through the miscibility gap, after contact with each solution, the concentration gradient becomes steeper due to spinodal decomposition. Based on Eq.(1), a spatially non-uniform concentration field, where the concentration gradient becomes steeper, creates transient interfacial tension and the interfacial tension would increase with the concentration gradient. Our experimental results show that when the system is partially miscible, interfacial tension increases with time, which indicates an increase in the concentration gradient and the non-uniformity of concentration with time. The temporal increase in interfacial tension indicates the occurrence of spinodal decomposition, which induces a spatial gradient (or non-uniformity) of the concentration in the bulk solution; this is more significant at the interface of both phases. As described by Mauri et al. [45,46] and Poesio et al. [47], the force produced under spinodal decomposition is referred to as the Korteweg force. This is thermodynamically defined as the functional derivative of free energy [46] and is characterized by a body force. This force produces spontaneous convection to minimize the free energy stored at an interface [45–51] and it has also been reported that a droplet moves spontaneously by such Korteweg force [45,47–51]. In the present study, we demonstrate that the observed fingering is caused by spontaneous convection of such the Korteweg force explained by Mauri et al. [45,46]. In the following, we show how this Korteweg forces can be understood for a fully miscible system. The interfacial tension γ in binary system in a

nonhomogeneous concentration field is defined as [42,43,52]

$$\gamma = k\int_{-\infty}^{\infty}\left(\frac{\partial c}{\partial x}\right)^2 dx \sim k\frac{(\Delta c)^2}{\delta}, \qquad (1)$$

where c is the concentration, k is the gradient energy parameter, x is coordinate normal to the interface, Δc is the difference in concentration between the two phases, and δ is the interface thickness. Since the concentration gradient creates a transient interfacial tension in partially miscible systems similar to fully miscible systems, we consider the equation (1) may be used for both fully and partially miscible systems. For a fully miscible system, δ constantly increases and Δc vanishes in the course of diffusion; therefore, the concentration gradient rapidly decays to zero. In fact, the interfacial tension shown in Fig. 2 (a) temporally decreases and approaches zero for the fully miscible system. This indicates that our experimental results are in good agreement with the theoretical model given in Eq (1) for a fully miscible system. Furthermore, studies on a fully miscible system [52–59] have shown that the effective interfacial tension (Korteweg stress) can also be written as an additional force in the momentum equation as the divergence of the Korteweg stress tensor, which can be termed as a body force as it depends on the concentration gradient in the bulk solution [53–59].

To evaluate the quantitative relation between the interfacial deformation and the physical properties, we define the interfacial deformation intensity, I_d, as a standard deviation—$I_d = \sqrt{\sum_{\theta=0}^{2\pi}\{R(\theta) - \langle R\rangle\}^2/N}$—of the interfacial radius $R(\theta)$, where $\langle\ \ \rangle$ denotes the average value and θ is an angle [Fig. 1(c)]. N is the number of samples of R (in this work, N = 1024). Fig. 3(a) shows that the deformation becomes larger as C_s is larger and it becomes smaller as q is larger.

Here, we propose a dimensionless number $\mathrm{B_f} = \Delta\gamma b^2/\eta q$ that represents the relative effect of the body force driven by thermodynamic instability versus the pressure gradient related by Darcy's law.

$$\mathrm{B_f} = \frac{\frac{\Delta\gamma}{2\pi r_{max} b}}{\frac{\eta V}{k}} = \frac{\Delta\gamma b^2}{\eta q}. \qquad (2)$$

We neglect the numerical coefficient on the right-hand side for simplicity. Here, $\Delta\gamma = \gamma^* - \gamma_0$, where γ^* and γ_0 are interfacial tension measured by the spinning drop method [Fig. 2(b)] at a time when r_{max} reaches 42 mm and at the beginning of the measurement, respectively, and k (=b^2/12) is permeability of Hele-Shaw cell and η is viscosity of the displacing solution. We emphasize that the temporal change in interfacial tension relates the body force driven by the thermodynamic instability, as described in the preceding paragraph. $\mathrm{B_f}$ = 0 corresponds to an immiscible system. In Fig. 3(b), we can find that $I_d/I_{d,Im}$ (I_d at various C_s normalized by I_d in the immiscible case for various q) against $\mathrm{B_f}$ falls on a universal curve. For $\mathrm{B_f} < 0$, which corresponds to a fully miscible system, no deformation was observed, whereas for $\mathrm{B_f} > 0$, which corresponds to a partially miscible system, $I_d/I_{d,Im}$ increased with increasing $\mathrm{B_f}$ regardless of q. The smaller interfacial deformation at high q is

due to the pressure gradient by fluid injection exerting a dominant influence over the thermodynamic body force.

To clarify the origin of the body force, we determine the thermodynamically unstable region. The system with compositions lying in the thermodynamically unstable region, that is, the spinodal region, becomes a partially miscible, whereas outside this region, it becomes a fully miscible. This region is determined by the following relation [60]:

$$G_{\mathrm{PP}}G_{\mathrm{WW}} - {G_{\mathrm{PW}}}^2 < 0, \qquad (3)$$

where $G_{\mathrm{PP}} = 1/r_{\mathrm{P}}\phi_{\mathrm{P}} + 1/r_{\mathrm{S}}\phi_{\mathrm{S}} - 2\chi_{\mathrm{PS}}$, $G_{\mathrm{WW}} = 1/\phi_{\mathrm{W}} + 1/r_{\mathrm{S}}\phi_{\mathrm{S}} - 2\chi_{\mathrm{SW}}$, and $G_{\mathrm{PW}} = 1/r_{\mathrm{S}}\phi_{\mathrm{S}} - \chi_{\mathrm{SW}} - \chi_{\mathrm{PS}} + \chi_{\mathrm{PW}}$ (ϕ_{i} is the volume fraction and indices P, W, and S denote PEG, water, and salt, respectively; r_{i} is the segment number of component *i*; and χ_{ij} represents the interaction parameters). χ_{ij} are determined by the Gibbs free energy of mixing of the Flory–Huggins theory [61]. The value of χ_{ij} used to calculate $G_{\mathrm{PP}}, G_{\mathrm{WW}}, G_{\mathrm{PW}}$ has been experimentally found based on the cloud-point measurement given in [62] which is obtained using a refractometer [63]. The relation between the spinodal region and $\mathrm{B_f}$ is shown in Fig. 3(c). The value of the left-hand side of equation (3) decreases with $\mathrm{B_f}$, and spinodal decomposition occurs when $\mathrm{B_f} > 0$ regardless of q corresponding to C_s > 12.3% w/w as shown in the inset. The spinodal region is consistent with the region in which interfacial deformation occurs. The result confirms that the body force is identified as Korteweg force driven by the thermodynamic instability and as the cause of the fingering instability during hydrodynamically stable displacement.

To confirm the occurrence of spontaneous convection by the Korteweg force and identify the chemical that triggers Korteweg force, we conduct the following experiment. After injecting the more viscous liquid into the less viscous one at a higher q to avoid interfacial deformation until the radius reached 20 mm in the radial Hele-Shaw cell, we stop injection and observe the temporal evolution of the circular interface. No deformation is seen in the immiscible and fully miscible cases [Fig. 4(a)]. However, for C_s = 19% w/w in the partially miscible case [Fig. 4(a)], a clear dimple is observable at 5 min. A droplet of the salt-rich solution forms from a dimple at 7 min and moves to the center of the circular pattern of the more viscous liquid. Such droplet motion by Korteweg force in ATPS has been reported experimentally and theoretically [49–51]. In addition, we find that the droplets never cross the center, indicating that they move in the direction of higher PEG concentration. As C_s increases, the onset time of the first droplet monotonically decreases [Fig. 4(b)]. These observations can be summarized as follows: (1) the spontaneous flow induced by Korteweg force is directed from the salt-rich solution toward the PEG-rich solution, that is, the flow is in the direction in which the PEG concentration gradient is positive; and (2) the magnitude of the flow monotonically increases with C_s. Due to such spontaneous convection from salt-rich phase to

PEG-rich phase, the interfacial fingering deformation occurs when more-viscous PEG solution displaces the less-viscous salt solution as shown in Fig.1(b). The dynamics without and with the injection are different because the flow exists in the latter cases. However, we claim here that the interface can be deformed without the injection in the partially miscible systems and the interface in immiscible and fully miscible systems are not changed. In short, the occurrence of the spontaneous convection induced in the partially miscible system is not dependent on the injection rates. Without the injection, the spontaneous convection is confirmed as the formation and movement of droplets. With the injection, such convection assists for the formation of the interfacial fingering

We calculate the components of Korteweg force K_{ij} from the gradient energy parameters κ_{ij} derived from χ_{ij} [64]. The details of the procedure for obtaining κ_{ij} are described by Ariyapadi and Nauman [64]. K_{ij} generated by the interaction between components *i* and *j* [48,65] are obtained as follows, assuming that the lengths of the spatial inhomogeneities are comparable to the interface thickness ($\delta \sim 100$ μm) [43];

$$K_{\mathrm{PW}} = \frac{1}{2}\kappa_{\mathrm{PW}}\nabla(\nabla\phi_{\mathrm{P}})^2 \sim \frac{1}{2}\kappa_{\mathrm{PW}}\frac{1}{\delta}\left(\frac{\phi_{\mathrm{P,i}}-\phi_{\mathrm{P,o}}}{\delta}\right)^2, \qquad (4)$$

$$K_{\mathrm{PS}} = \kappa_{\mathrm{PS}}\nabla^2\phi_{\mathrm{P}}\nabla\phi_{\mathrm{S}} \sim \kappa_{\mathrm{PS}}\frac{1}{\delta}\left(\frac{\phi_{\mathrm{P,i}}-\phi_{\mathrm{P,o}}}{\delta}\right)\left(\frac{\phi_{\mathrm{S,i}}-\phi_{\mathrm{S,o}}}{\delta}\right), \qquad (5)$$

$$K_{\mathrm{SW}} = \frac{1}{2}\kappa_{\mathrm{SW}}\nabla(\nabla\phi_{\mathrm{S}})^2 \sim \frac{1}{2}\kappa_{\mathrm{SW}}\frac{1}{\delta}\left(\frac{\phi_{\mathrm{S,i}}-\phi_{\mathrm{S,o}}}{\delta}\right)^2, \qquad (6)$$

where $\phi_{\mathrm{i,o}}$ and $\phi_{\mathrm{i,i}}$ are the concentrations of component *i* in the outer and inner liquids, respectively, and the direction from the salt-rich solution toward the PEG-rich solution is positive. Here, we emphasize that Eqs. (4)–(6) state that Korteweg force is driven by compositional gradients. Note that δ, which is determined by intermolecular interaction [48,65], affects the absolute values of K_{ij} but not the ratio between them. All components of the calculated K_{ij} are shown in Fig. 4(c). The force generated by the interaction between PEG and water, K_{PW}, increases with C_s. This force component constitutes 96.0%–99.8% of the total force. Thus, the direction of the PEG concentration gradient determines the direction of net spontaneous convection by Korteweg force. This theoretical finding qualitatively agrees with experimental observations (1) and (2) described above.

Here, we emphasize that the change in the interfacial tension does not always indicate the presence of the Marangoni effect and that the Marangoni effect is not responsible for interfacial deformation. We thermodynamically control the miscibility of two aqueous solutions by varying their salt concentration, thereby allowing systematically changes in the interfacial tension and its dynamics. The Marangoni effect occurs when a surface-active agent is adsorbed on the interface, and a concentration gradient is generated. In our systems, the surface-active agent is PEG; however, its concentration is almost constant in all experimental systems. The adsorption of PEG molecules on the interface did not directly induce a change in the interfacial tension. In fact, the change in the

miscibility of the two aqueous solutions induced changes in the interfacial tension. In general, the Marangoni number is defined in terms of the amount of change in interfacial tension as a function of the concentration of the surface-active agent in equilibrium. Thus, instead of the Marangoni number, we used the dimensionless number B_f in terms of the amount of temporal change in interfacial tension due to spinodal decomposition under nonequilibrium conditions, indicating the generation of a body force (Korteweg force).

Furthermore, we note that this deformation is not caused by buoyancy-driven instability because the displacement experiment in 14% w/w Na_2SO_4 shows more deformation than that in the immiscible system [Fig. 3(a)] although the density difference in 14% w/w Na_2SO_4 (0.070 $g \cdot cm^{-3}$) is smaller than those in the immiscible system (0.084 $g \cdot cm^{-3}$).

IV Conclusion

In conclusion, we have demonstrated that partial miscibility can trigger fingering even under hydrodynamically stable displacement; this is because of spontaneous convection by Korteweg force. Our experiments show that the fingering instability in partially miscible systems is governed by the newly proposed dimensionless number B_f. For $B_f > 0$, the interfacial deformation is proportional to B_f. For negative values of B_f, deformation never occurs despite the same absolute value of temporal change in the interfacial tension. Hence, it is observed that the sign of B_f is a crucial factor for the development of the interface. The results in this study are completely different from those of other fingering phenomena under hydrodynamically stable conditions in immiscible and fully miscible systems described in the introductory paragraph. Further, the fingering phenomenon described herein is the first one whose origin is not the establishment of a local positive viscosity gradient or a local negative permeability gradient under hydrodynamically stable conditions in standard Hele–Shaw cells. This discovery will directly contribute to CO_2-EOR technology where there is a process in which more viscous water displaces less viscous CO_2, which would be partially miscible. Our fingering phenomena indicate that displacements considered to be hydrodynamically stable could be unstable in these processes. From a scientific viewpoint, the present study opens a new cross-disciplinary research area between hydrodynamics and chemical thermodynamics, that is, interfacial hydrodynamics involving Korteweg force originating during phase separation in partially miscible systems [66,67].

Acknowledgements

The authors would like to thank Mr. Keisuke Morita for his assistance with the cloud point measurements. This work was supported by PRESTO-JST (No. 25103004 “Phase Interfaces for Highly Efficient Energy Utilization”). M.M. was also supported by JSPS Invitation Fellowships for Research in Japan (No. S15063).

Figure and Table captions

Fig.1 (a) Phase diagram of PEG 8000–Na_2SO_4–water system (from Ref. [40]) and solution systems used in the present study. The solutions used in the immiscible, fully miscible, and partially miscible systems are indicated by red, black, and green circles, respectively. (b) Hydrodynamically stable displacement in the immiscible, fully miscible, and partially miscible systems for $q = q_0$. The pictures are taken when the longest radius of the displacement pattern is 42 mm and the injection time is shown at the lower right corner of each picture. (c) Time evolution of the patterns for $q = q_0$. The lines of different colors indicate t = 100, 300, 500, 1000, 1500, 2000, and 2500 s.

Fig.2 (a) Interfacial rheological measurement for the immiscible (phase L−phase H system), fully miscible (36.5% w/w PEG–0% w/w Na_2SO_4 system), and partially miscible (36.5% w/w PEG–20% w/w Na_2SO_4system) systems. (b) Typical time evolution of interfacial tension for immiscible, fully miscible (36.5% w/w PEG–9% w/w Na_2SO_4 system), and partially miscible systems. The rotation rate of the capillary is 6000 rpm.

Fig.3 (a) Intensity of deformation, I_d, vs C_s for various q. The separate graph on the right is for the immiscible case. (b) $I_d/I_{d,Im}$ vs $\mathrm{B_f} = \Delta\gamma b^2/\eta q$. (c) $G_{\mathrm{PP}}G_{\mathrm{WW}} - {G_{\mathrm{PW}}}^2$ vs $\mathrm{B_f}$. (inset) $G_{\mathrm{PP}}G_{\mathrm{WW}} - {G_{\mathrm{PW}}}^2$ vs C_s. The region in which its value is negative corresponds to the spinodal region.

Fig.4 (a) Temporal variation of the circular interface between the two fluids in the immiscible, fully miscible, and partially miscible systems (C_s = 19% w/w). (b) Onset time of the first dimple vs. C_s. (c) as a function of C_s.

Table 1 Viscosity and density of solutions used

[1] B. S. Broyles, R. A. Shalliker, D. E. Cherrak, and G. Guiochon, Visualization of viscous fingering in chromatographic columns, J. Chromatogr. A **822**, 173 (1998).

[2] J. M. Nordbotten, M. A. Celia, and S. Bachu, Injection and storage of CO2 in deep saline aquifers: Analytical solution for CO2 plume evolution during injection, Transp. Porous Media **58**, 339 (2005).

[3] L. W. Lake, R. T. Johns, W. R. Rossen, and G. A. Pope, Fundamentals of Enhanced Oil Recovery, *Fundamentals of Enhanced Oil Recovery* (Society of petroleum engineers, Richardson, TX, 2014).

[4] P. G. Saffman and G. Taylor, The Penetration of a Fluid into a Porous Medium or Hele-Shaw Cell Containing a More Viscous Liquid, Proc. R. Soc. A **245**, 312 (1958).

[5] S. Hill, Channeling in packed columns, Chem. Eng. Sci. **1**, 247 (1952).

[6] R. L. Chuoke, P. Van Meurs, and C. Van der Poel, The instability of slow, immiscible, viscous liquid-liquid displacements in permeable media, Pet. Trans. AIME **216**, 188 (1959).

[7] G. M. Homsy, Viscous Fingering in Porous Media, Annu. Rev. Fluid Mech. **19**, 271 (1987).

[8] K. V. McCloud and J. V. Maher, Experimental perturbations to Saffman-Taylor flow, Phys. Rep. **260**, 139 (1995).

[9] J. D. Chen, Radial viscous fingering patterns in Hele-Shaw cells, Exp. Fluids **5**, 363 (1987).

[10] J. D. Chen, Growth of radial viscous fingers in a Hele-Shaw cell, J. Fluid Mech. **201**, 223 (1989).

[11] J. Nittmann, G. Daccord, and H. E. Stanley, Fractal growth of viscous fingers: quantitative characterization of a fluid instability phenomenon, Nature **314**, 141 (1985).

[12] G. Daccord, J. Nittmann, and H. E. Stanely, Radial viscous fingering and diffusion-limited aggregation: Fractal dimension and growth sites, Phys. Rev. Lett. **56**, 336 (1986).

[13] E. Lemaire, P. Levitz, G. Daccord, and H. Van Damme, From viscous fingering to viscoelastic fracturing in colloidal fluids, Phys. Rev. Lett. **67**, 2009 (1991).

[14] H. Zhao and J. V. Maher, Associating-polymer effects in a Hele-Shaw experiment, Phys. Rev. E **47**, 4278 (1993).

[15] A. De Wit and G. M. Homsy, Nonlinear interactions of chemical reactions and viscous fingering in porous media, Phys. Fluids **11**, 949 (1999).

[16] J. Fernandez and G. M. Homsy, Viscous fingering with chemical reaction: Effect of in-situ production of surfactants, J. Fluid Mech. **480**, 267 (2003).

[17] Y. Nagatsu, K. Matsuda, Y. Kato, and Y. Tada, Experimental study on miscible viscous fingering involving viscosity changes induced by variations in chemical species concentrations due to chemical reactions, J. Fluid Mech. **571**, 475 (2007).

[18] Y. Nagatsu, S. K. Bae, Y. Kato, and Y. Tada, Miscible viscous fingering with a chemical reaction involving precipitation, Phys. Rev. E **77**, 067302 (2008).

[19] Y. Nagatsu, A. Hayashi, M. Ban, Y. Kato, and Y. Tada, Spiral pattern in a radial displacement

involving a reaction-producing gel, Phys. Rev. E **78**, 026307 (2008).

[20] F. Haudin, J. H. E. Cartwright, F. Brau, and A. De Wit, Spiral precipitation patterns in confined chemical gardens, Proc. Natl. Acad. Sci. United State Am. **111**, 17363 (2014).

[21] F. Haudin and A. De Wit, Patterns due to an interplay between viscous and precipitation-driven fingering, Phys. Fluids **27**, 113101 (2015).

[22] M. Mishra, P. M. J. Trevelyan, C. Almarcha, and A. De Wit, Influence of Double Diffusive Effects on Miscible Viscous Fingering, Phys. Rev. Lett. **105**, 204501 (2010).

[23] M. Ahmadlouydarab, J. Azaiez, and Z. Chen, Immiscible flow displacements with phase change in radial injection, Int. J. Multiph. Flow **72**, 73 (2015).

[24] C. K. Chan and N. Y. Liang, Observations of Surfactant Driven Instability in a Hele-Shaw Cell, Phys. Rev. Lett. **79**, 4381 (1997).

[25] H. Tang, W. Grivas, D. Homentcovschi, J. Geer, and T. Singler, Stability considerations associated with the meniscoid particle band at advancing interfaces in Hele-Shaw suspension flows, Phys. Rev. Lett. **85**, 2112 (2000).

[26] F. Xu, J. Kim, and S. Lee, Particle-induced viscous fingering, J. Nonnewton. Fluid Mech. **238**, 92 (2016).

[27] J. Kim, F. Xu, and S. Lee, Formation and Destabilization of the Particle Band on the Fluid-Fluid Interface, Phys. Rev. Lett. **118**, 074501 (2017).

[28] R. Krechetnikov and G. M. Homsy, On a new surfactant-driven fingering phenomenon in a Hele-Shaw cell, J. Fluid Mech. **509**, 103 (2004).

[29] J. Fernandez, R. Krechetnikov, and G. M. Homsy, Experimental study of a surfactant-driven fingering phenomenon in a Hele-Shaw cell, J. Fluid Mech. **527**, 197 (2005).

[30] I. Bihi, M. Baudoin, J. E. Butler, C. Faille, and F. Zoueshtiagh, Inverse Saffman-Taylor Experiments with Particles Lead to Capillarity Driven Fingering Instabilities, Phys. Rev. Lett. **117**, 034501 (2016).

[31] T. Podgorski, M. C. Sostarecz, S. Zorman, and A. Belmonte, Fingering instabilities of a reactive micellar interface, Phys. Rev. E **76**, 016202 (2007).

[32] T. Gérard and A. De Wit, Miscible viscous fingering induced by a simple A+B→C chemical reaction, Phys. Rev. E **79**, 016308 (2009).

[33] Y. Nagatsu and A. De Wit, Viscous fingering of a miscible reactive A + B → C interface for an infinitely fast chemical reaction: Nonlinear simulations, Phys. Fluids **23**, 043103 (2011).

[34] L. A. Riolfo, Y. Nagatsu, S. Iwata, R. Maes, P. M. J. Trevelyan, and A. De Wit, Experimental evidence of reaction-driven miscible viscous fingering, Phys. Rev. E **85**, 015304(R) (2012).

[35] Y. Nagatsu, Y. Ishii, Y. Tada, and A. De Wit, Hydrodynamic fingering instability induced by a precipitation reaction, Phys. Rev. Lett. **113**, 024502 (2014).

[36] X. Fu, L. Cueto-Felgueroso, and R. Juanes, Thermodynamic coarsening arrested by viscous

fingering in partially miscible binary mixtures, Phys. Rev. E **94**, 033111 (2016).

[37] M. A. Amooie, M. R. Soltanian, and J. Moortgat, Hydrothermodynamic mixing of fluids across phases in porous media, Geophys. Res. Lett. **44**, 3624 (2017).

[38] X. Fu, L. Cueto-Felgueroso, and R. Juanes, Viscous fingering with partially miscible fluids, Phys. Rev. Fluids **2**, 104001 (2017).

[39] F. M. J. Orr and J. J. Taber, Use of Carbon Dioxide in Enhanced Oil Recovery, Science (80-.). **224**, 563 (1984).

[40] S. M. Snyder, K. D. Cole, and D. C. Sziag, Phase Compositions, Viscosities, and Densities for Aqueous Two-Phase Systems Composed of Polyethylene Glycol and Various Salts at 25 °C, J. Chem. Eng. Data **37**, 268 (1992).

[41] S. Vandebril, A. Franck, G. G. Fuller, P. Moldenaers, and J. Vermant, A double wall-ring geometry for interfacial shear rheometry, Rheol. Acta **49**, 131 (2010).

[42] J. A. Pojman, C. Whitmore, M. L. T. Liveri, R. Lombardo, J. Marszalek, R. Parker, and B. Zoltowski, Evidence for the existence of an effective interfacial tension between miscible fluids: Isobutyric acid - Water and 1-butanol- water in a spinning-drop tensiometer, Langmuir **22**, 2569 (2006).

[43] B. Zoltowski, Y. Chekanov, J. Masere, J. A. Pojman, and V. Volpert, Evidence for the Existence of an Effective Interfacial Tension between Miscible Fluids. 2. Dodecyl Acrylate-Poly(dodecyl acrylate) in a Spinning Drop Tensiometer, Langmuir **23**, 5522 (2007).

[44] R. Mauri, R. Shinnar, and G. Triantafyllou, Spinodal decomposition in binary mixtures, Phys. Rev. E **53**, 2613 (1996).

[45] D. Molin, R. Mauri, and V. Tricoli, Experimental evidence of the motion of a single out-of-equilibrium drop, Langmuir **23**, 7459 (2007).

[46] D. Molin and R. Mauri, Enhanced heat transport during phase separation of liquid binary mixtures, Phys. Fluids **19**, 074102 (2007).

[47] P. Poesio, G. P. Beretta, and T. Thorsen, Dissolution of a liquid microdroplet in a nonideal liquid-liquid mixture far from thermodynamic equilibrium, Phys. Rev. Lett. **103**, 064501 (2009).

[48] N. Vladimirova, A. Malagoli, and R. Mauri, Diffusiophoresis of two-dimensional liquid droplets in a phase-separating system, Phys. Rev. E **60**, 2037 (1999).

[49] T. Ban, A. Aoyama, and T. Matsumoto, Self-generated Motion of Droplets Induced by Korteweg Force, Chem. Lett. **39**, 1294 (2010).

[50] T. Ban, T. Yamada, A. Aoyama, Y. Takagi, and Y. Okano, Composition-dependent shape changes of self-propelled droplets in a phase-separating system, Soft Matter **8**, 3908 (2012).

[51] T. Ban, T. Fukuyama, S. Makino, E. Nawa, and Y. Nagatsu, Self-Propelled Vesicles Induced by the Mixing of Two Polymeric Aqueous Solutions through a Vesicle Membrane Far from Equilibrium, Langmuir **32**, 2574 (2016).

[52] D. Truzzolillo, S. Mora, C. Dupas, and L. Cipelletti, Off-equilibrium surface tension in colloidal suspensions, Phys. Rev. Lett. **112**, 128303 (2013).

[53] I. Kostin, M. Marion, R. Texier-Picard, and V. A. Volpert, Modelling of miscible liquids with the Korteweg stress, Math. Model. Numer. Anal. **37**, 741 (2003).

[54] C. Y. Chen, L. Wang, and E. Meiburg, Miscible droplets in a porous medium and the effects of Korteweg stresses, Phys. Fluids **13**, 2447 (2001).

[55] C. Y. Chen, Numerical simulations of fingering instabilities in miscible magnetic fluids in a Hele-Shaw cell and the effects of Korteweg stresses, Phys. Fluids **15**, 1086 (2003).

[56] C. Y. Chen and H. J. Wu, Numerical simulations of interfacial instabilities on a rotating miscible magnetic droplet with effects of Korteweg stresses, Phys. Fluids **17**, 042101 (2005).

[57] S. Swernath, B. Malengier, and S. Pushpavanam, Effect of Korteweg stress on viscous fingering of solute plugs in a porous medium, Chem. Eng. Sci. **65**, 2284 (2010).

[58] S. Pramanik and M. Mishra, Linear stability analysis of Korteweg stresses effect on miscible viscous fingering in porous media, Phys. Fluids **25**, 074104 (2013).

[59] S. Pramanik and M. Mishra, Nonlinear simulations of miscible viscous fingering with gradient stresses in porous media, Chem. Eng. Sci. **122**, 523 (2015).

[60] L. Yilmaz and A. J. Mchugh, Analysis of Nonsolvent -Solvent -Polymer Phase Diagrams and Their Relevance to Membrane Formation Modeling, J. Appl. Polym. Sci. **31**, 997 (1986).

[61] I. G. Sargantanis and M. N. Karim, Prediction of Aqueous Two-Phase Equilibrium Using the Flory-Huggins Model, Ind. Eng. Chem. Res. **36**, 204 (1997).

[62] K. Morita, Effect of distance from equilibrium on spontaneous defromation of droplet driven by Korteweg force, Effect of Distance from Equilibrium on Spontaneous Defromation of Droplet Driven by Korteweg Force, Osaka University, 2013.

[63] M. Mohsen-Nia, H. Rasa, and H. Modarress, Cloud-point measurements for (water + poly(ethylene glycol) + salt) ternary mixtures by refractometry method, J. Chem. Eng. Data **51**, 1316 (2006).

[64] M. V. Ariyapadi and E. B. Nauman, Gradient energy parameters for polymer polymer solvent systems and their application to spinodal decomposition in true ternary systems, J. Polym. Sci. Part B Polym. Phys. **28**, 2395 (1990).

[65] B. Zhou and A. C. Powell, Phase field simulations of early stage structure formation during immersion precipitation of polymeric membranes in 2D and 3D, J. Memb. Sci. **268**, 150 (2006).

[66] S. Tsuchitani, T. Fukutake, D. Mukai, H. Miki, and K. Kikuchi, Unstable Spreading of Ionic Liquids on an Aqueous Substrate, Langmuir **33**, 11040 (2017).

[67] Y. Chao, S. Y. Mak, Q. Ma, J. Wu, Z. Ding, L. Xu, and H. C. Shum, Emergence of Droplets at the Nonequilibrium All-Aqueous Interface in a Vertical Hele-Shaw Cell, Langmuir **34**, 3030 (2018).

Fig.1

(a)

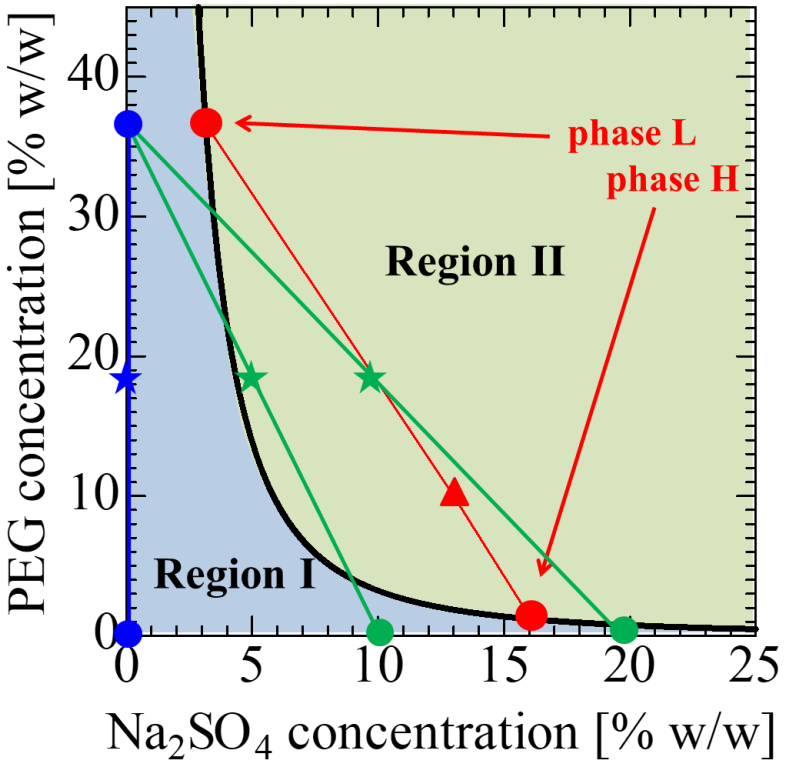
PEG concentration [% w/w]
40
30
20
10
0
0
5
10
15
20
25
Na_2SO_4 concentration [% w/w]
phase L
phase H
Region II
Region I

(b)

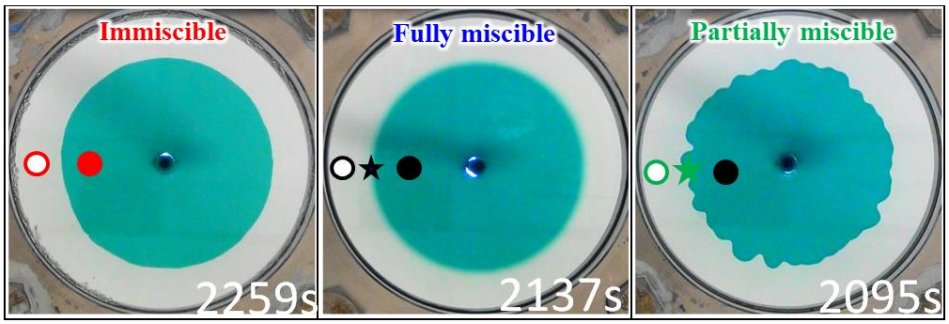
Immiscible
Fully miscible
Partially miscible
2259s
2137s
2095s

(c)

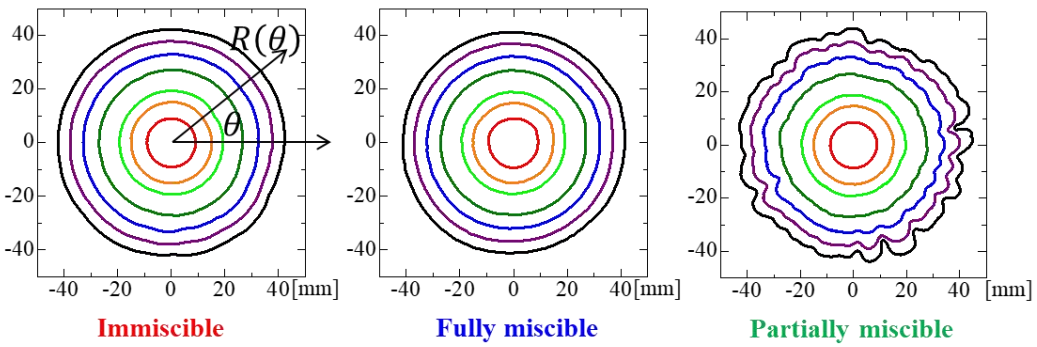
$R(\theta)$
θ
40
20
0
-20
-40
-40 -20 0 20 40[mm]
-40 -20 0 20 40 [mm]
Immiscible
Fully miscible
Partially miscible

Fig.2

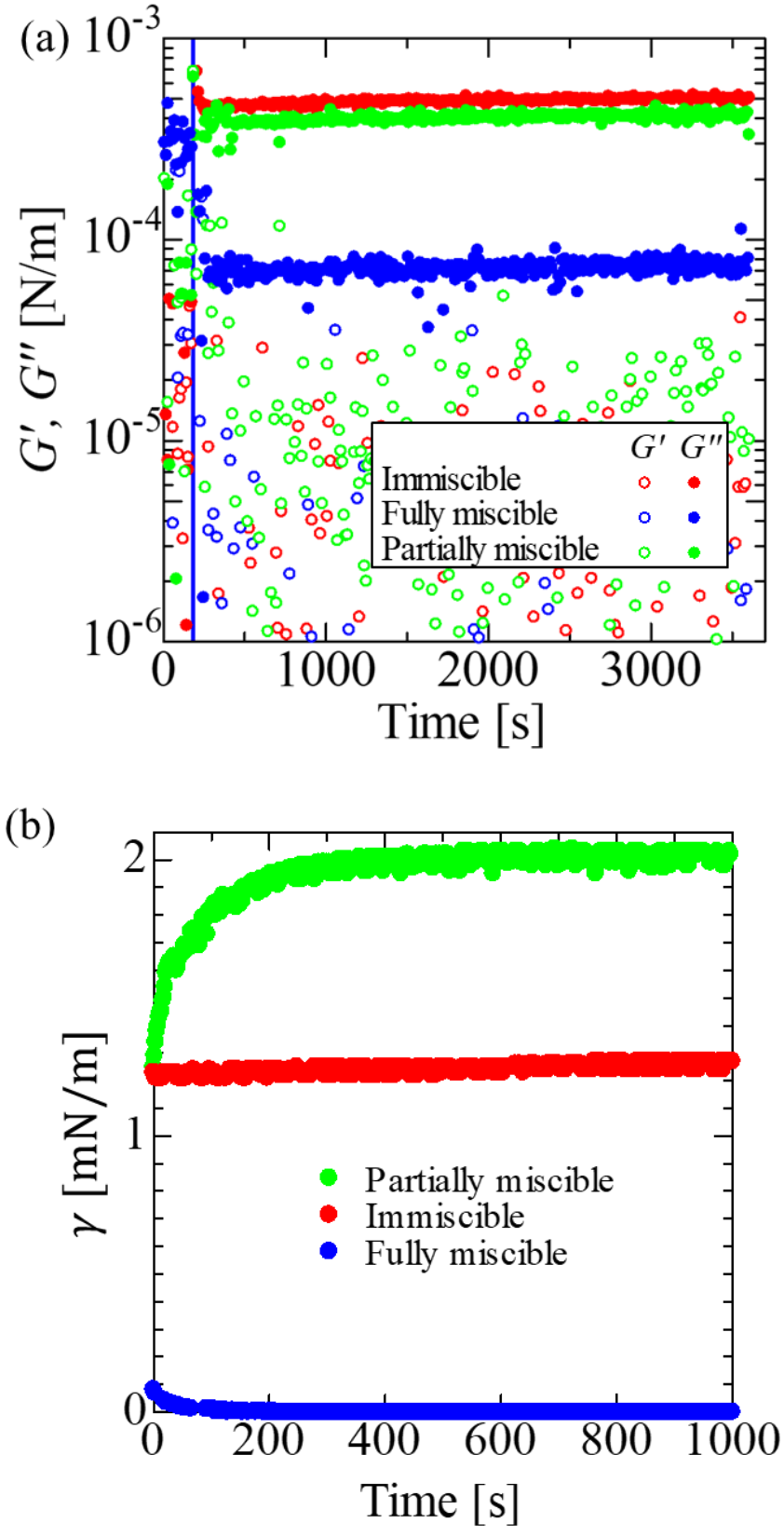
(a)
10^{-3}
10^{-4}
10^{-5}
10^{-6}
G', G'' [N/m]
G' G''
Immiscible
Fully miscible
Partially miscible
0
1000
2000
3000
Time [s]
(b)
2
1
0
γ [mN/m]
Partially miscible
Immiscible
Fully miscible
0
200
400
600
800
1000
Time [s]

Fig.3

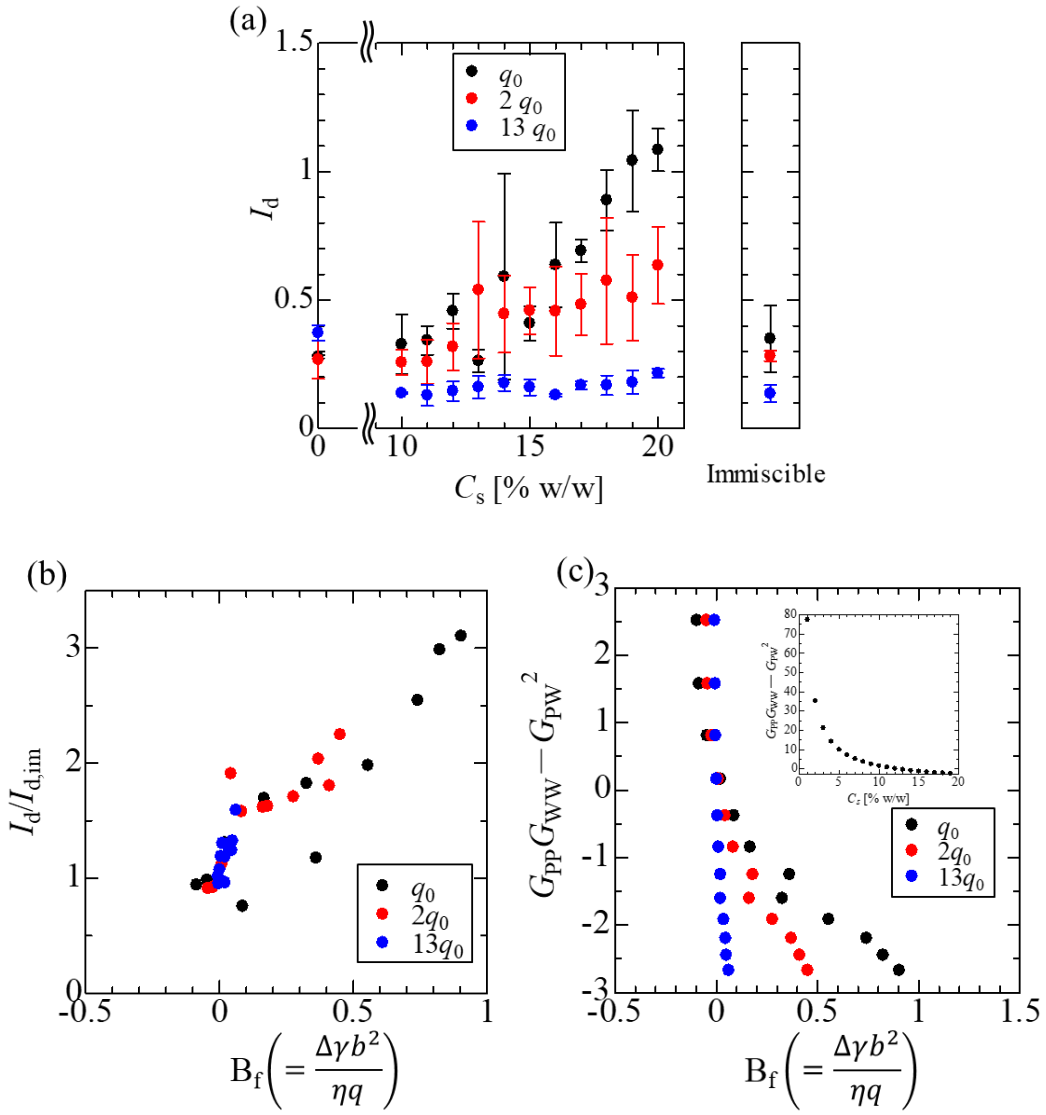
(a)
I_d
C_s [% w/w]
Immiscible
q_0
2 q_0
13 q_0
(b)
$I_d/I_{d,im}$
$B_f\left(=\frac{\Delta\gamma b^2}{\eta q}\right)$
(c)
$G_{PP}G_{WW}-G_{PW}^2$
$B_f\left(=\frac{\Delta\gamma b^2}{\eta q}\right)$
C_s [% w/w]

Fig.4

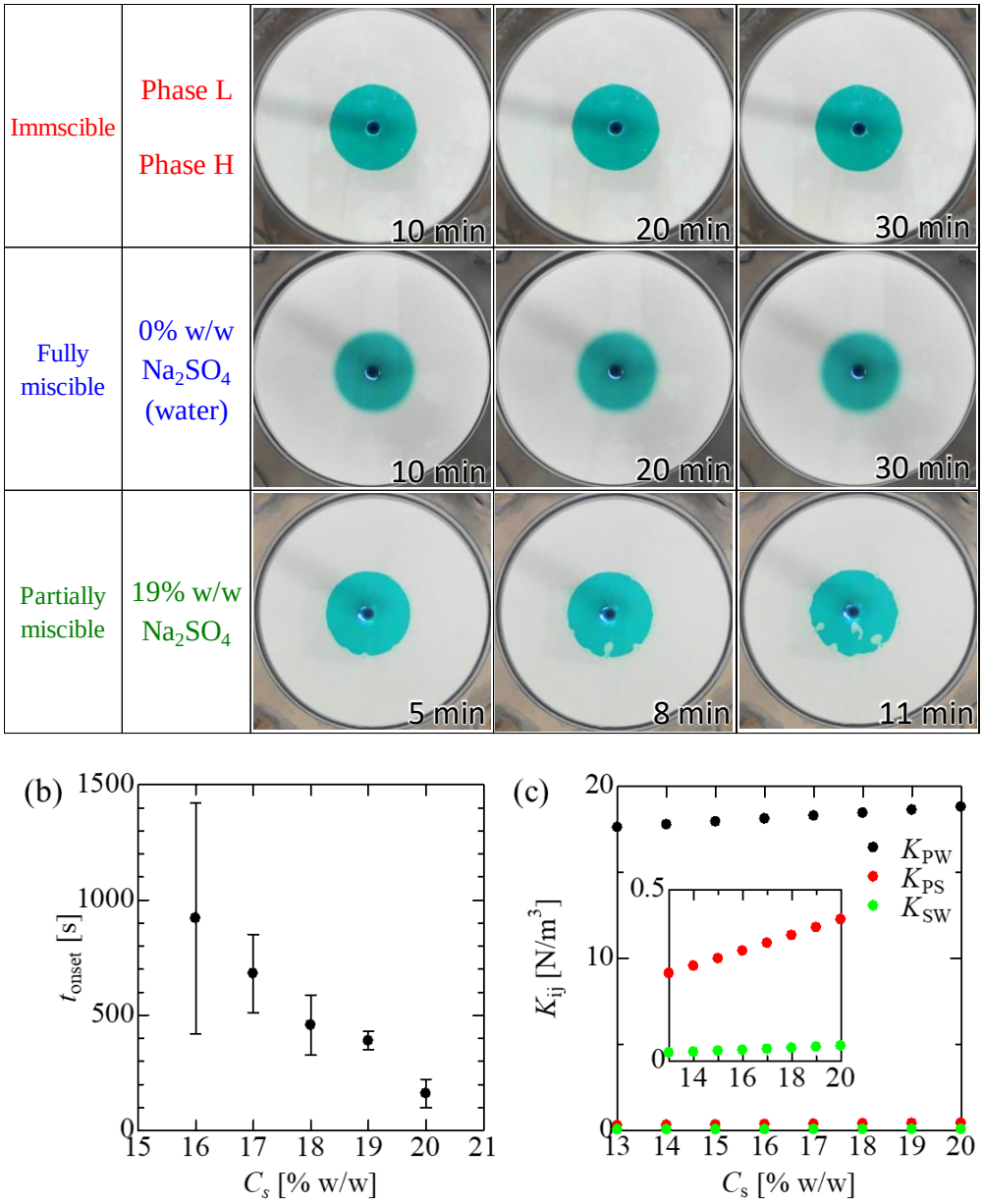

Table 1

	Viscosity [mPa·s]	Density [g/cm^3]
36.5% w/w PEG	112	1.07
0% w/w Na_2SO_4*	0.972	0.997
15% w/w Na_2SO_4	1.65	1.14
19% w/w Na_2SO_4	1.92	1.18
20% w/w Na_2SO_4	2.08	1.19
Phase L	125	1.08
Phase H	1.76	1.16

*0 wt% Na_2SO_4 represents deionized water.